PHYSICAL REVIEW C VOLUME 27, NUMBER 6 JUNE 1983

Unified analysis of pionic atoms and low-energy pion-nuclear scattering: Hybrid analysis

R. Seki
Department of Physics and Astronomy, California State University, Northridge, California 91330
and W. K. Kellogg Radiation Laboratory, California Institute of Technology, Pasadena, California 91125

K. Masutani* and K. Yazaki
Department of Physics, Faculty of Science, University of Tokyo, Bunkyō-ku, Tokyo, Japan
(Received 2 August 1982)

Using the method of effective nuclear density, we apply a simple, π-nucleus optical potential (without ρ^2 terms and the Lorentz-Lorenz effect) to π^- atoms and low-energy π-nucleus elastic scatterings. Data of both phenomena are analyzed in a unified, hybrid (phenomenological and theoretical) manner: The π^--atom data are analyzed first to determine phenomenologically the potential parameters at threshold. The parameters are then extrapolated successfully up to 50 MeV incident pion laboratory energy by a microscopic calculation in which the energy-dependence correction is made after including the Fermi-averaging and Pauli-blocking effects. In contrast to other work, our potential includes the minimum number of the parameters that describe the full information content of the data. We can thus conclude that these effects are the important microscopic corrections for the extrapolation, but neither the Lorentz-Lorenz effect nor some highly nonlocal effects are crucial ones. The potential we have used has angular transformation terms which are also found to be crucial in the unified treatment. During the course of this work we have found an interesting behavior of the terms. A short account of its discussion is also presented.

[NUCLEAR REACTIONS Unified analysis and calculation; strong-interaction shifts and widths in π^- atoms and differential cross sections of elastic π-nucleus scattering up to 50 MeV; π-nucleus optical potential.]

I. INTRODUCTION

Bunatyan and Pol'[1] (hereafter referred to as JINR) and Stricker *et al.* (Refs. 2 and 3 referred to as MU1 and MSU2, respectively) have demonstrated an interesting, simultaneous description of both π^- atoms and low-energy π-nucleus scatterings. Though they extend their analyses to higher energy regions, we concentrate here on the region up to about 50 MeV. In their work the π-nucleus optical potential of Ericson and Ericson[4] that fits π^--atom data is shown to be also capable of reproducing low-energy scattering data after some modifications. The major modifications include the energy dependence of the coefficient of ρ (=nuclear density distribution) and the effect due to angular transformation terms (ATT).[5] However, MSU1 included the former only in the imaginary parts and JINR used the π^--atom potential parameters that were obtained without ATT. As to the coefficients of ρ^2, MSU1 assumed $\mathrm{Re}B_0=-\mathrm{Im}B_0$ and $\mathrm{Re}C_0=-\mathrm{Im}C_0$, and JINR assumed $\mathrm{Re}B_0=\mathrm{Re}C_0=0$, both using the full Lorentz-Lorenz effect $\xi=1$, and MSU2 tried to incorporate a theoretical calculation of these parameters with a few values of $\xi>1$. As pointed out in the preceding paper, the low-energy data (π^- atoms and π-nucleus scattering) are insensitive to details of the π-nucleus optical potential. In particular, the potential of Ericson-Ericson is too complicated for all the parameters to be determined phenomenologically. As was done in these works, one way to handle this problem is to fix some parameters to the values judged to be the best and to assign their energy dependence, based on some theoretical reasoning. Since the potential form of Ericson-Ericson seems to include most of the significant physics and to be the most convenient as a description of the low-energy phenomena, this way of handling the problem may be considered to be quite reasonable and, in fact, these authors are successful in the extrapolation of this potential from the threshold (the π^- atoms) to the low-energy scattering. However, because there are too many parameters and too much uncertainty, it is not clear what is really the essential physics responsible for the successful extrapolation.

Although the data are insensitive to the details of the potential, they do determine the effective parameter values rather reliably, as discussed in the preceding paper. Thus care must be taken so that, when some parameters are fixed in the way mentioned above, the final set of the parameters does yield the correct effective parameter values. For example, we found that the parameters proposed by MSU1 do not reproduce the π^--atom data well. The chi-square per degree of freedom (χ^2/N) that we obtained is about 17 for their set 1 and about 14 for their set 2 by using the π^--atom data without including the new, accurate data. Certainly the exact values of χ^2/N vary depending on the choice of the nuclear densities, but these values of χ^2/N appear quite large.

In view of these situations, we decided, by following the preceding paper,[6](1) to use an effective potential which has the minimum number of parameters needed to represent the data; (2) to determine the parameter values by a rigorous best-fit search to the π^--atom data; and then (3) to extrapolate these parameters up to 50 MeV scattering with the least number of corrections including the most significant physics based on a simple, clearcut microscopic theory. As was the case in the other work mentioned above, this method is also a hybrid one, being a combination of phenomenological and theoretical calculations. But in our work the two parts of the calculations are clearly separated and care is taken to avoid as much phenomenological and theoretical ambiguity as possible.

Based on the work described in the preceding paper, the effective potential is constructed by exploiting the facts that the insensitivity of the data manifests itself in correlations between the coefficients of ρ and ρ^2 in the potential and that the correlations are approximately independent of the atomic mass number and vary slowly as the pion energy increases. Therefore, our effective potential is simply proportional to ρ without ρ^2 terms and the Lorentz-Lorenz effect. In this form of the potential we include the ATT because it has a kinematic rather than a dynamic origin (as a consequence of transformation from the π-nucleon c.m. system to the π-nucleus c.m. system) and also because it has been shown[5] to be important in scattering problems. The potential is referred to as the MKIS (modified Kisslinger) in the preceding paper and has as a form for $\pi^{\pm}$

$$2\bar{\mu}V^{\pm}(r)=4\pi p_1(b_0\rho\mp b_1\delta\rho)-4\pi\{c_0(\vec{\nabla}\rho\cdot\vec{\nabla}-\epsilon\vec{\nabla}^2\rho)\mp c_1(\vec{\nabla}\delta\rho\cdot\vec{\nabla}-\epsilon\vec{\nabla}^2\delta\rho)\}/p_1\ , \tag{1}$$

where, in terms of the proton (ρ_p) and neutron (ρ_n) densities, ρ and $\delta\rho$ are defined as $\rho=\rho_n+\rho_p$ and $\delta\rho=\rho_n-\rho_p$. We also define the kinematic factors as $p_1=1+2\epsilon$ and

$$\epsilon=(\mu^2+K^2)^{1/2}/2m$$

in terms of the pion (μ) and nucleon (m) masses and of the π-nucleus c.m. ($\approx\pi$ lab) momentum k. $\bar{\mu}$ is the reduced pion mass of the system. In Eq. (1) the ATT are those with $\vec{\nabla}^2$.

We emphasize that the reason to use this simple form of the potential is not that it is a realistic potential, but because it is a practical one. That is, the detailed structure of the MKIS may not be physical, but it serves the purpose of reproducing the elastic data (i.e., the shifts and widths in the π^- atoms, and the scattering cross sections of the complicated π-nucleus interaction). In this sense it is an effective potential and the parameters are the effective parameters.

The major part of this work was reported[7] at the 8th International Conference on High Energy Physics and Nuclear Structure (Vancouver, 1979) and its short version has appeared[8] as a Letter. After this work was completed, we were informed about MSU2. As described above and in the Introduction of the preceding paper, MSU2 and our work deal with the same topic but differ in the way it is investigated: Apart from the fact that MSU2 uses the Ericson-Ericson potential while we use the MKIS, MSU2 merely reports an observation of the effective parameters, while in our work they are the crux of our unification of the π^--atom and scattering data. As seen in the following sections, we report a careful, systematic treatment of the effective potential using the effective density and also a clear conclusion as to which microscopic effects are really essential in such a unification.

II. ANGULAR TRANSFORMATION TERMS (ATT)

Before we proceed to discuss the details of our analysis, let us describe an interesting property of the ATT which we found. The quantitative feature of what we are going to describe certainly depends on our choice of the potential form, but we believe that the qualitative feature is common to other forms of the potential.

In order to examine the property of the ATT, we first generated π^--atom data shifts and widths with and without the ATT and examined the differences between the two. The potential parameter set used for this comparison is the best fit to 59 π^--atom data without the ATT, and is listed in the first

column of Table I. We observed that the ATT is *attractive* in all states of the π^- atoms, decreasing the magnitude of $1s$ shifts by a few to about 10%, and increasing the magnitude of higher state shifts by a greater amount, near 20%. Little effect was observed on the widths. We repeated the same procedure on the $\pi^{\pm}$-^{12}C scatterings by comparing the partial wave scattering amplitudes for 30—50 MeV. When the ATT are included, the magnitude of the negative real part of the s-wave amplitude was observed to increase by nearly 50%, but the magnitudes of the positive real parts of the higher-wave amplitude were observed to increase only by at most 5%. The changes in the imaginary parts were seen to be generally small. Thus in these scattering energies the ATT becomes *repulsive* for $l=0$, but attractive for $l>0$. We illustrate the behavior of the s-wave amplitude in Fig. 1.

This effect, being repulsive and attractive above and below the threshold, respectively, for $l=0$, while attractive throughout for $l>0$, is easily understood when we examine the behavior of the ATT as a function of r. As can be observed in Eq. (1), the real part of the ATT is not zero only in the region of the nuclear surface, being positive inside and turning negative at R a little beyond the half nuclear-density radius, as shown in Fig. 2. Note that in the case of two parameter Fermi distributions proportional to

$$\{1+\exp[4\ln 3(r-c)/t]\}^{-1},$$

we have

$$R=c(1+\eta^2-\tfrac{2}{3}\eta^{4+}\cdots),$$

where $\eta=(8\ln 3)t/c$. In the case of the π^- atoms the atomic wave function behaves as r^l for $l>0$, while for $l=0$ it is pushed out by the repulsive (and also absorptive) local interaction. Thus the contribution from the negative region of the ATT outweighs that from the positive region so as to yield the *attractive* effect. On the other hand, for the scattering energies of our interest the value of kR is rather close to $\pi/2$ (about 1.5 even for ^{12}C at 30 MeV). As seen in the unperturbed form of the wave function $j_0(kr)$, the inner repulsive becomes strong so as to yield the net *repulsive* effect. As for $l>0$, the centrifugal barrier again pushes out the wave function and the outer attraction dominates. In the case of light nuclei such as ^{12}C and ^{16}O, the null effect of the ATT on the s wave was numerically found to occur at about 15 MeV above the threshold for π^+ and at a little less than 10 MeV for π^-, as seen in Fig. 1. In heavier nuclei the energy tends to be higher for π^+ and lower for π^-, and the ATT can change sign more than once owing to a complicated distortion of the wave function. We feel that, because of its strong energy dependence, the ATT effect may not be evaluated reliably by comparing the π-nucleus scattering length, as was done by MSU1.

Before closing the discussion on the ATT effect, we wish to clarify the strength of this effect. In the above comparison of the atomic-level shifts and phase shifts with and without the ATT, we observed a significant difference in the energy shifts of $l>0$ atomic states and in $l=0$ scattering phase shifts. These shifts are a consequence of two opposing effects of the local and nonlocal parts of the potential, as illustrated by their sign changes in the p-state atomic shift for large nuclei and in the s-wave phase shift at a higher energy. A large difference is thus created by upsetting the appreciable cancellation between two effects. As seen in the following, the inclusion of the ATT changes the best-fit potential-parameter values only by a little (generally, $\lesssim 10\%$).

III. THE MKIS PARAMETERS

In the preceding paper we analyzed the π^--atom data using the Kisslinger form of the potential

TABLE I. Optical potential parameters at the threshold for the Kisslinger form of the potential (KIS) and for the modified Kisslinger form [as shown in Eq. (1), MKIS]. The π^--atom parameters are the best fit to 59 atoms and the free π-nucleon values are taken from Rowe, Salomon, and Landau (Ref. 11). Errors using the KIS are practically the same as those using the MKIS.

		π^- atom		
		KIS	MKIS	Free π nucleon
$\mathrm{Re}b_0$	(μ^{-1})	0.0285	0.0310±0.0007	0.0037
$\mathrm{Im}b_0$	(μ^{-1})	−0.0102	−0.0103±0.0006	0.000
b_1	(μ^{-1})	0.12	0.14 ±0.02	0.094
$\mathrm{Re}c_0$	(μ^{-3})	−0.173	−0.163 ±0.004	−0.230
$\mathrm{Im}c_0$	(μ^{-3})	−0.016	−0.019 ±0.002	0.000
c_1	(μ^{-3})	−0.17	−0.20 ±0.03	−0.151
χ^2/N		3.0	2.9	

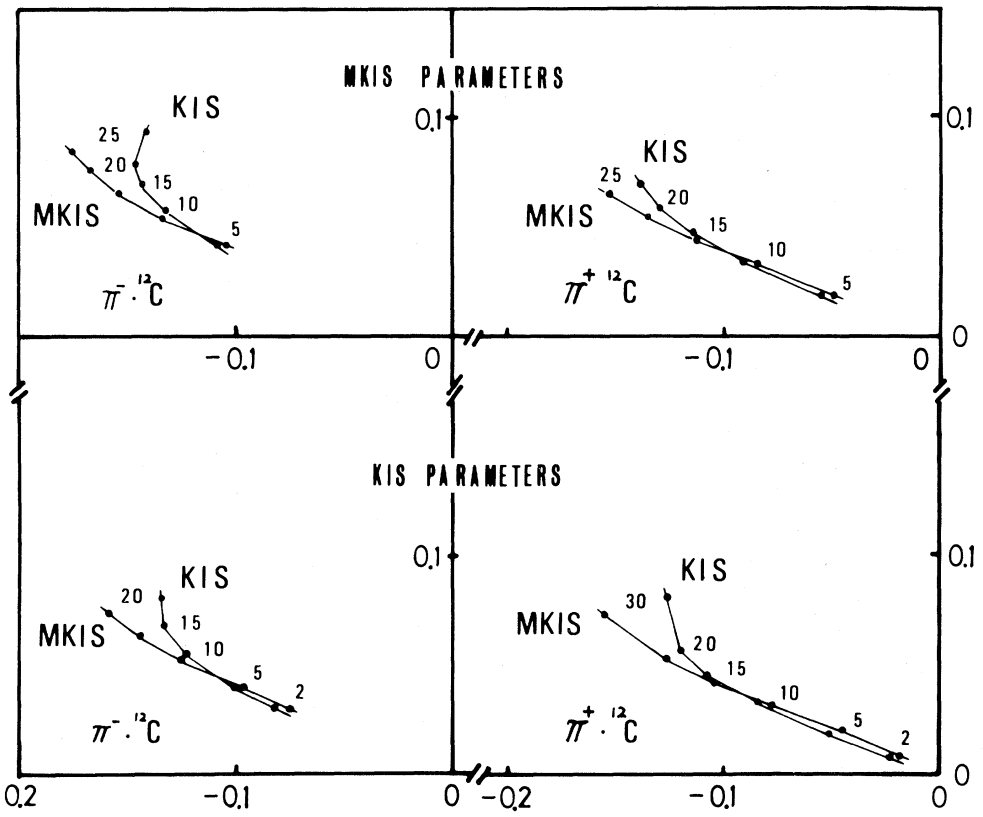

FIG. 1. Argand diagrams for the s-wave $\pi^{\pm}$-^{12}C scattering amplitude with (MKIS) and without (KIS) the angular transformation terms (ATT). In each case the MKIS and KIS parameters fitted to the π^--atom data are used, and the results are denoted as MKIS parameter and KIS parameter, respectively. When the MKIS and KIS curves cross in each figure, the ATT has the null effect.

without the ATT. In order to carry out a consistent analysis of the low-energy phenomena, we reanalyzed the data using the MKIS. As discussed in Sec. III of the preceding paper, the isoscalar parameters have been found to be approximately the same in the analyses of different sets of data, but the isovectors have been found to be rather difficult to determine, even including the new data[9] that have been reported in the last few years. It has also been observed that the new data yield large χ^2/N values of 4–5 while the old data yield 2–4, and that the origin of such an increase has not been explained. Under these circumstances and also for the sake of convenience of comparison, we continued to use in this analysis the old data set of 59 π^- atoms described in the preceding paper. (A further, critical discussion on the isovector parameters using the new data will be given in Sec. IV in connection with a comparison to π-scattering data for $N > Z$ nuclei.) Using these π^--atom data, the best-fit potential parameters were searched in the same way as described in Sec. III of the preceding paper. The parameters values thus found are listed in the second column of Table I, labeled MKIS. In Table I the difference between the second column and the first column (labeled KIS) corresponds to the effect of

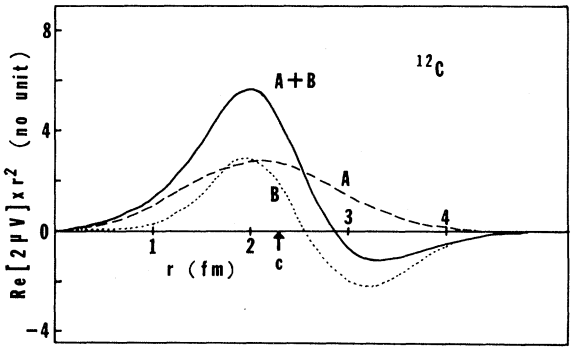

FIG. 2. The radial variation of the real part of the modified Kisslinger (MKIS) potential for ^{12}C. Curve A is the Kisslinger (KIS) local part of the potential, curve B is the angular transformation terms (ATT), and curve $A+B$ is a sum of the two, the full MKIS (local part) potential. Note that the radial integration of curve B is zero.

the ATT at the threshold. As discussed in Sec. II, the ATT contribute as attractive; therefore the repulsive parameter b_0 increases and the attractive parameter c_0 decreases in magnitude so as to accommodate the ATT contribution.

In order to use the potential parameters in low-energy scattering we must correct them for changes which occur because of an increase in the pion energy (T_π). We do this by adding to the MKIS parameters *the difference* of the π-nucleon amplitudes in the nuclear medium that are evaluated at $T_\pi > 0$ and $T_\pi = 0$. In this way the energy dependence of the quasielastic scattering part is taken into account, but the inelastic scattering part, such as two-nucleon absorption, is not properly included. The latter process is known to cause a somewhat weak energy dependence in the potential parameters as a result of the kinematics. When this part of the energy dependence is included by following a parametrization given by Landau and Thomas,[10] we notice some variation in the differential cross sections. However, from the restricted amount of the presently available data on the process $\pi^+ + d \to p + p$, we cannot make the partial-wave decomposition unambiguously and thus cannot determine precisely how large a change occurs in the individual parameters as the energy increases. Furthermore, the quantities whose energy dependences are in question are not just the coefficients of say, $\rho^2(r)$, but the effective coefficients of $\rho(r)$ including a part of $\rho^2(r)$ after $\rho^2(r)$ is interpreted as $\rho(r)$ times the effective density. Because so much ambiguity is thus involved, we decided not to include the energy dependence in the absorption process.

The bound π-nucleon amplitudes are determined by evaluating a relation

$$\tau = t + t(G - G_0)\tau \,, \tag{2}$$

where t and τ are the free and bound π-nucleon t matrices, respectively. G_0 and G are the π-nucleon Green's functions in free space and in the nuclear medium, respectively. Using the Fermi gas model, we evaluated Eq. (2) by including the effect of Pauli blocking (the PBE) and Fermi averaging (the FAE). We show the details of the calculation in Appendix A. As the free π-nucleon amplitudes, we used the analytic forms given by Rowe, Salomon, and Landau.[11] The Fermi momentum p_F used is the one evaluated by the effective density at the threshold, $\rho_e(0)$, rather than p_F evaluated by the nuclear matter density $\rho_0 = 0.5\mu^3$. The bound π-nucleon amplitudes therefore depend on ρ_e through the choice of p_F.

In Fig. 3 we show the real part of the s-wave-bound-π-nucleon amplitude thus calculated, in comparison to the free π-nucleon amplitude. We see that a cusp at the threshold practically disappears in the bound π-nucleon amplitude. The disappearance of the cusp is due to the inclusion of the PBE and corresponds to the fact that the Pauli exclusion principle makes the amplitude less singular by eliminating the leading singularity at the threshold. We emphasize that the threshold cusp does not disappear if we evaluate an expression obtained by terminating the series expansion of Eq. (2),

$$\tau = t + t(G - G_0)t + t(G - G_0)t(G - G_0)t + \cdots \,,$$

after a finite number of terms. We suspect that this mechanism of the disappearance of the threshold cusp in the bound amplitude is known among some workers in this field, but we are not aware of any previous work which explicitly points out the mechanism. (The other mechanism discussed[10] is going off-shell by including the binding energy of the nucleon.) Therefore, partly for pedagogical purposes, we present a simple, demonstrative proof of the mechanism in Appendix B.

Let us make a further technical remark: As we have seen so far, the PBE is a crucial medium correction, as is apparent from its role of removing the threshold cusp. On the other hand, the FAE can be shown to be a small effect in this low-energy region except for the p-wave imaginary part, whose energy dependence is rather strong near the threshold. Actually, it is a somewhat complicated matter to assess the significance of the FAE because the FAE in our calculation does not appear separately, but rather enters in an evaluation of the PBE as a momentum averaging as well as an energy averaging. The method of Appendix A includes the PBE with the FAE, while that of Appendix B includes only the PBE, basically because of the static approximation. The amplitudes calculated by two methods are generally numerically close, but differ noticeably in the p-wave imaginary part, because in the method of Appendix B the PBE is evaluated at a fixed energy and fails to include a contribution from the rapidly increasing imaginary part on the higher energy side. In the actual calculations which will be discussed in the next section, we used the method of Appendix A.

Once the bound π-nucleon amplitudes are determined at a given energy, we compute the potential parameters using the relation for b_0

$$b_0(T_\pi) = b_0(\text{atom}) + \Delta(T_\pi) \,, \tag{3}$$

where

$$\Delta(T_\pi) = b_0^c(T_\pi, \rho_e(0)) - b_0^c(0, \rho_e(0)) \,, \tag{4}$$

and also using similar relations for other parameters. Here $b_0^c(T_\pi, \rho_e(0))$ is the calculated potential parameter which equals the negative of the bound π-nucleon amplitude (described above). In Eq. (4)

we explicitly show the $\rho_e(0)$ dependence because we wish to discuss in Sec. V a subtle ambiguity caused by the choice of ρ_e with which b_0^c is calculated.

As seen in Fig. 3, once the PBE is included, b_0^c is practically a linear function of T_π. Since the energy-dependence correction, $\Delta(T_\pi)$, equals the difference of the b_0^c's at T_π and 0, $\Delta(T_\pi)$ can be set, as a good approximation, to be the difference at $T_\pi+\epsilon$ and ϵ for some small ϵ. The same statement is also applicable tc other potential parameters. It is known[10,12] that the nuclear binding effect is mostly accounted for by evaluating the amplitudes at the proper three-body energy, which is somewhat lower than the actual scattering energy. Therefore, we expect that the nuclear binding effect is negligible *in the energy dependence correction after the PBE is included,* and we do not consider this effect any further. We here emphasize our points, that, in short, the nuclear binding effect is energy independent once the PBE is included and that this binding effect may contribute significantly to the amplitudes themselves at a given energy, but in our calculation this contribution is already included in the phenomenological threshold values.

Let us summarize what we have discussed so far in this section. In order to extrapolate the potential parameters which are phenomenologically determined at the threshold, we add to them the energy-dependence corrections, $\Delta(T_\pi)$'s. As indicated in Eq. (4), $\Delta(T_\pi)$ is the difference between the amplitude (times the minus sign) at T_π and 0 *after the PBE with the FAE is included.* Throughout the rest of this paper we simply refer to this complicated correction with the PBE and the FAE $\Delta(T_\pi)$ as "the energy-dependence correction," unless specified otherwise.

Taking the example of ^{12}C at $T_\pi=50$ MeV, we show in Table II the size of the energy-dependence corrections to the parameters that have to be made in order to extrapolate to low-energy scattering. In Table III the extrapolated (MKIS) values and the phenomenological values at 50 MeV obtained in the preceding paper are shown for comparison. The extrapolated values happen to be in very good agree-

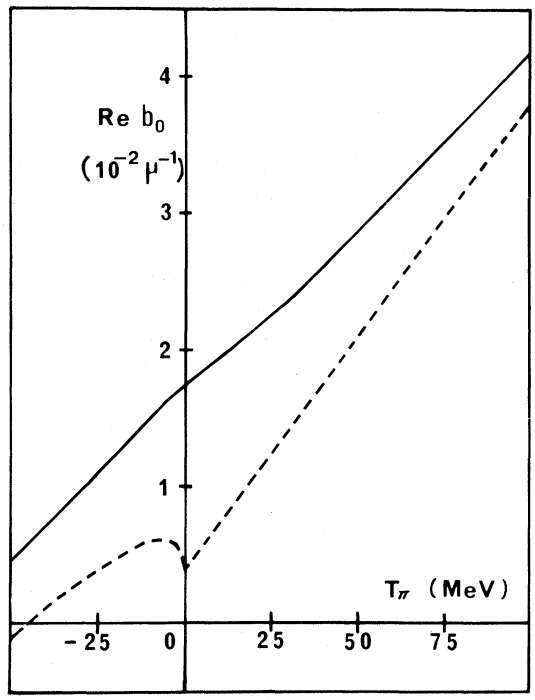

FIG. 3. The potential parameter $\mathrm{Re}b_0$ as a function of the pion energy T_π. The broken curve is the free π-nucleon scattering amplitude of Ref. 8 with the minus sign. The continuous curve is the parameter calculated from this amplitude, including the Pauli-blocking and Fermi-averaging effects in the method of Appendix A.

TABLE II. The energy-dependence corrections to be made for an extrapolation from the threshold to 50 MeV. Δ (free, 50 MeV) is a correction directly computed from the free π-nucleon amplitude without the PBE and the FAE. Δ (50 MeV) is the correction including the PBE and FAE according to the method of Appendix A (as discussed in Sec. III) and is used in the actual calculations. Δ′ (50 MeV) is another possible value shown for comparison, as discussed in Sec. V.

		Δ (free, 50 MeV)	Δ (50 MeV)	Δ′ (50 MeV)
$\mathrm{Re}b_0$	(μ^{-1})	0.0175	0.010	0.014
$\mathrm{Im}b_0$	(μ^{-1})	−0.0137	−0.006	−0.004
$\mathrm{Re}b_1$	(μ^{-1})	−0.0016	0.003	0.002
$\mathrm{Im}b_1$	(μ^{-1})	0.0036	0.001	0.001
$\mathrm{Re}c_0$	(μ^{-3})	−0.035	−0.019	−0.012
$\mathrm{Im}c_0$	(μ^{-3})	−0.032	−0.005	−0.004
$\mathrm{Re}c_1$	(μ^{-3})	−0.009	−0.002	−0.003
$\mathrm{Im}c_1$	(μ^{-3})	−0.016	−0.002	−0.002

TABLE III. Optical potential parameters at 50 MeV. The MKIS parameters are the hybrid analysis values and were used to compute the final results. They equal the MKIS value of Table I plus Δ (50 MeV) of Table II. The Phenom. I is the best-fit parameters to the 49.0 MeV π^+-^{12}C data using the MKIS and the Phenom. II is an average of the best fits to the π^+-^{12}C, -^{16}O, and -^{40}Ca scatterings near 50 MeV also using the MKIS.

		MKIS	Phenom. I	Phenom. II
$\mathrm{Re}b_0$	(μ^{-1})	0.041±0.004	0.043±0.002	0.045±0.001
$\mathrm{Im}b_0$	(μ^{-1})	−0.016±0.002	−0.012±0.003	−0.005±0.002
b_1	(μ^{-1})	0.14 ±0.02		
$\mathrm{Re}c_0$	(μ^{-3})	−0.18 ±0.01	−0.188±0.002	−0.192±0.005
$\mathrm{Im}c_0$	(μ^{-3})	−0.024±0.003	−0.02±0.01	−0.036±0.005
c_1	(μ^{-3})	−0.20±0.03		
χ^2/N				

ment with the phenomenological values in this case. Note that, as shown in Table II, our corrections to the imaginary part of the isovector parameters are relatively small. Since we had already set the isovector parameters to be real in the π^--atom analysis, we decided to discard these corrections to the imaginary parts.

The energy dependence corrections thus calculated have imaginary parts whose magnitudes increase slowly from zero at the threshold as the energy increases. Since we have neglected the energy dependence in the imaginary part due to the pion absorption, these imaginary parts represent quasielastic scatterings. Therefore, within our approximation a quantity

$$|\delta(\mathrm{Im}b_0)+\delta(\mathrm{Im}c_0)\vec{k}^{\,2}|/|\mathrm{Im}b_0+(\mathrm{Im}c_0)\vec{k}^{\,2}|$$

is a crude estimate of the ratio of the quasielastic and absorption cross sections. Here, $\vec{k}$ is an effective (local) pion momentum defined to be

$$\vec{k}^{\,2}\equiv-\langle\vec{\nabla}\rho\cdot\vec{\nabla}\rangle/\langle\rho\rangle\ ,$$

where $\langle\rho\rangle$ denotes an expectation value of ρ and a similar value for $\langle\vec{\nabla}\rho\cdot\vec{\nabla}\rangle$. δ denotes an increase from the threshold value, and $\mathrm{Im}b_0$ and $\mathrm{Im}c_0$ in the denominator are the threshold values. The above quantity is independent of the nuclear species (but $N\approx Z$) and thus the ratio of two cross sections must be independent of them. Using the parameter values at 50 MeV in Table I we find that the ratio is about 1/3. These results roughly agree with a more detailed calculation of the MSU1, and we feel that such agreement provides further evidence of the soundness of our approach.

IV. COMPARISON TO SCATTERING DATA

In Fig. 4(a), using an example of the π^+-^{12}C scattering at 50 MeV, we illustrate how the ATT and the energy-dependence corrections improve the agreement with the data. We observe that, while the ATT brings the first dip forward to about the observed location, the energy-dependence corrections raise the cross section closer to the data at the angles beyond the dip. Our final result including these corrections is shown in the figure as a continuous curve labeled MKIS. This final result of ours tends to be smaller around the plateau in large angles, but it is difficult to assess this tendency because various small effects other than those we have considered would contribute to the cross sections at these angles. Our assessment is then that the overall fit is reasonable and that the hybrid calculation is reliable for light isoscalar nuclei. In Fig. 4(b) we also show our prediction of the π^--^{12}C scattering at 50 MeV.

In Figs. 5–7 we show further comparisons with the data using only our final results of the calculation, i.e., with the ATT and the energy-dependence correction. For the π^+-^{12}C scattering the agreement between the calculation and the data is also good in the energies below 50 MeV, as shown in Figs. 5(a) and 6. A similarly good agreement is also achieved in scatterings from heavier, isoscalar nuclei, as demonstrated in Fig. 7 for the case of ^{40}Ca. As illustrated in Fig. 5(b) for the π^--^{12}C scattering at 30 MeV, the agreement seems somewhat better in the case of π^- scattering.

While the agreement is good for these $N=Z$ nuclei, we found that our calculation shows some disagreement with the data for heavy $N>Z$ nuclei. Figure 8 shows (as curve A) the π^+-^{208}Pb cross sections at 50 MeV using the hybrid (MKIS) parameters of Table III. We observe that the calculated dip is deeper and the calculated cross sections at large angles are smaller than the ones observed. The major reason for the disagreement seems to be the isovector parameters, which are poorly determined by the π^--atom data. The isovector parameter values used in this calculation are $(b_1,\ c_1)=(0.14\mu^{-1},$

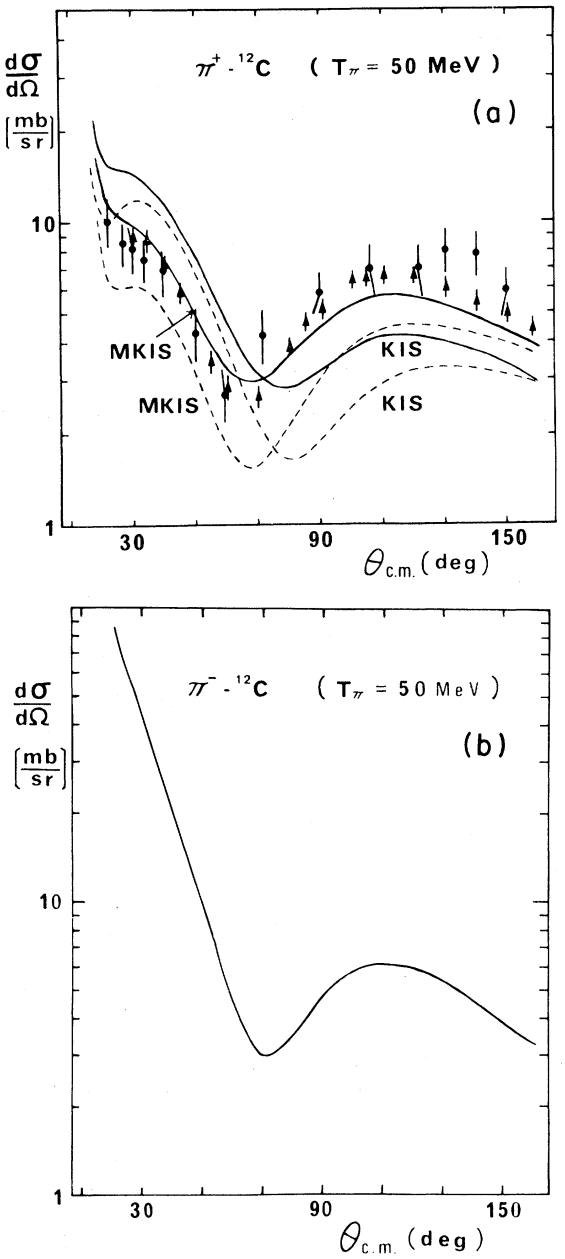

FIG. 4. (a) Effects of the energy dependence correction, Δ (50 MeV), and the angular transformation terms in π^+-^{12}C elastic scattering cross section at 50 MeV. Dotted curves are the cross section calculated using the π^--atom parameters, and solid curves are those calculated including Δ (50 MeV) and the energy dependence correction with the Pauli-blocking and Fermi averaging effects. The MKIS refers to the KIS plus the angular transform terms. [See Eq. (1).] The data at 49.9 MeV are from LAMPF (Ref. 13) and at 48.9 MeV from TRIUMF (Ref. 14). (b) π^--^{12}C elastic scattering cross section at 50 MeV calculated using the modified Kisslinger potential (MKIS) with the energy-dependence correction including the Pauli-blocking and Fermi-averaging effects.

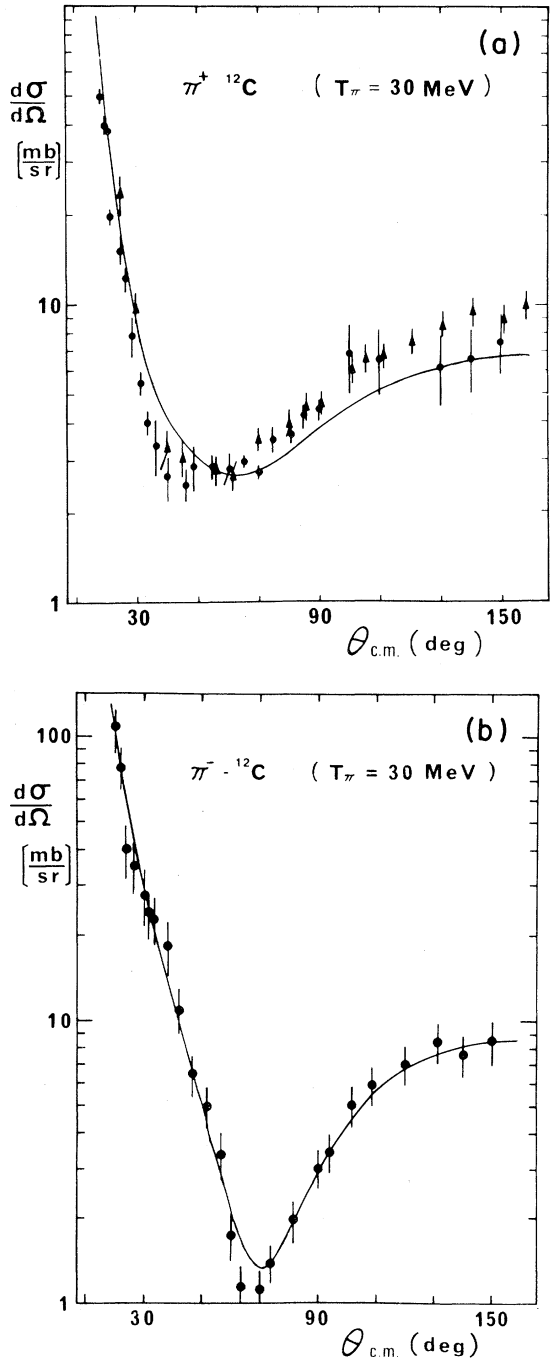

FIG. 5. (a) π^+-^{12}C elastic scattering cross section at 30 MeV calculated as in Fig. 4(b). The data are also at 30 MeV (Ref. 15). (b) π^--^{12}C elastic scattering cross section at 30 MeV calculated as in Fig. 4(b). The data are at 29 MeV (Ref. 16).

$-0.20\mu^{-3}$) as shown in Table III, while the best-fit phenomenological values are $(0.06\mu^{-1}, -0.16\mu^{-3})$, as given in Table IV of the preceding paper.

In fact, the major portion of the difference could

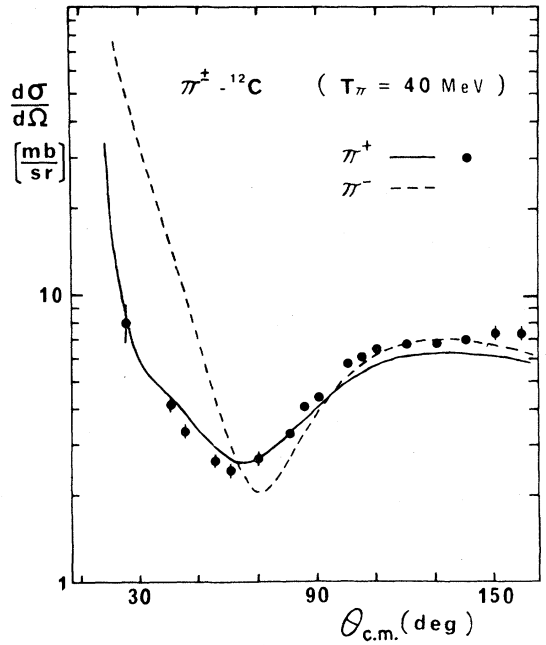

FIG. 6. $\pi^{\pm}$-^{12}C elastic scattering cross section at 40 MeV calculated as in Fig. 4(b). The π^+ are also at 40 MeV (Ref. 17).

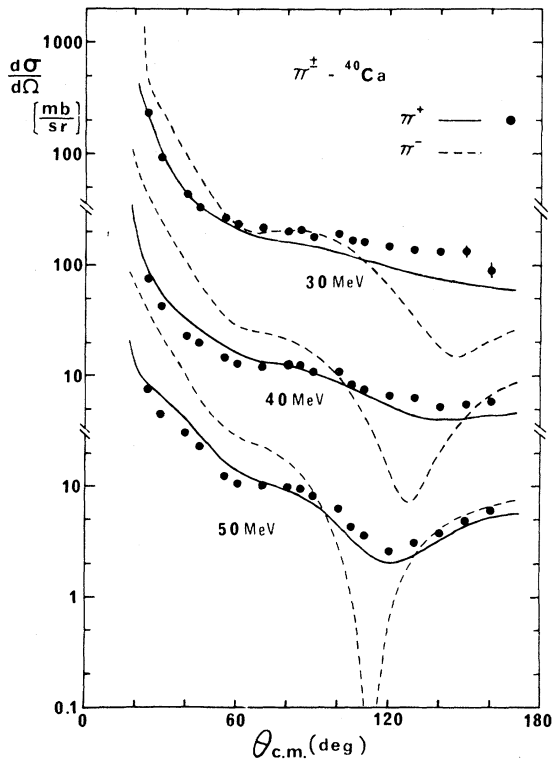

FIG. 7. $\pi^{\pm}$-^{40}Ca elastic scattering cross section at 30, 40, and 50 MeV calculated as in Fig. 4(b). The π^+ data are also at 30 and 50 MeV (Ref. 15) and at 40 MeV (Ref. 17).

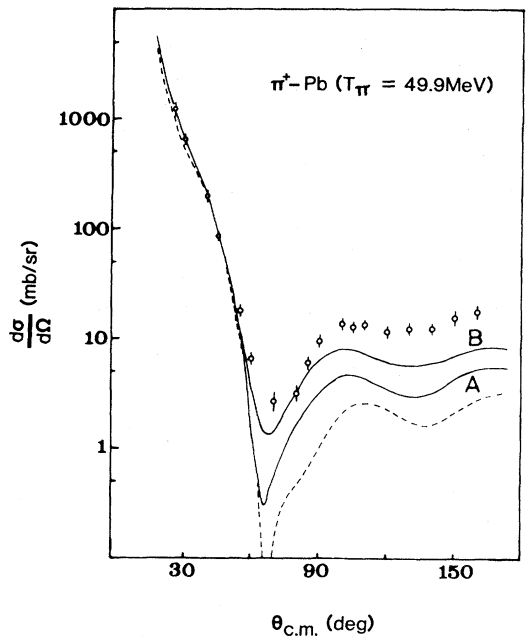

FIG. 8. Influence of the new b_1 value (obtained from new π^--atom 1s-state data) on π^+-^{208}Pb scattering at 49.9 MeV. Curve A is obtained using the hybrid MKIS parameters of Table III and curve B is calculated using the new b_1 value fitted to new π^--atom data in the 1s state together with the c_1 value fitted to the π^--^{208}Pb atom data. (See the text for details.) The dotted curve is calculated using the potential parameters fitted to the 59 π^--atom data without any energy-dependence correction and is shown for the purpose of comparison. The data are from Ref. 15.

be accounted for using more realistic isovector-parameter values, particularly for b_1. For example, we tried $(b_1, c_1)=(0.08\mu^{-1}, -0.15\mu^{-3})$, which are rather close to the best-fit values, and Fig. 8 indeed shows (curve B) that these parameter values yield a better agreement with the data. Let us describe how we chose these values: After our calculation described so far had been completed, some new π^--atom data in the 1s state were reported by a Basel group[18] and a TRIUMF group.[19] The new data include an accurate ^{18}O datum[18] which is substantially different from the old, less accurate one. We noted in the previous paper that the old ^{18}O datum had always contributed a large χ^2 in our fittings and that we had been suspicious of the datum. The other newly reported data include those[19] for $N\neq Z$ nuclei of ^{3}He, ^{11}B, and ^{13}C. Being the datum for the $N-Z=2$ nucleus with the largest A among these nuclei, the ^{18}O datum has an important role in the phenomenological determination of the b_1 parameter. In order to investigate the π^+-^{208}Pb scattering problem, we decided to take $b_1=0.08\mu^{-1}$ from very

recent analyses by Friedman and Gal[20] and Friedman[21] rather than to redo our entire π^--atom analysis. In these new analyses the new data are used with a more realistic ρ_n (i.e., with $\rho_n/N \neq \rho_p/Z$) but unfortunately altogether only six π^- atoms in the $1s$ and $2p$ are used for the actual fitting and no data for heavy nuclei are used. We therefore find the c_1 value by fitting to the π^--^{208}Pb atom data[22] using the same isoscalar parameter values as the hybrid MKIS values (at 50 MeV) in Table I. The c_1 value turns out to be $-0.15\mu^3$. Here we did not make the energy-dependence corrections to the b_1 and c_1 values because our nuclear matter calculation of Table II shows the corrections to the isovector parameters to be small (though we are aware of limitations in extrapolating a result of such a calculation to $N > Z$ nuclei).

Actually, Table III shows an inequality,

$$b_1/\mathrm{Re}b_0 \gg c_1/\mathrm{Re}c_0 ,$$

to hold. Therefore, the crucial parameter is b_1 in the sense that a change in the b_1 value influences the cross sections more significantly than the same (percent) change in the c_1 value does. In fact, we observe that, even if c_1 is varied by several tens of percent, the cross sections do not change appreciably and that, once the b_1 value is properly chosen, even the use of a different ρ_n $[\neq(N/Z)\rho_p]$ does not substantially alter the good agreement with the π^+ scattering data (but not with the π^- scattering data, as discussed later in this section). Note that we do not, of course, imply that the precise value of c_1 cannot be determined phenomenologically: It can be, once ρ_n and ρ_p are known, and vice versa.

We illustrate the above observation in Fig. 9, which shows two curves C and D in comparison to curve B that is identical to curve B in Fig. 8. Curves C and D differ from curve B in the use of a more realistic $\rho_n \neq (N/Z)\rho_p$ of ^{208}Pb: Curves B and C use the same potential parameters, but a more realistic ρ_n of ^{208}Pb is used for the computation of curve C while, as explained previously, $\rho_n = (N/Z)\rho_p$ is used for curve B. Curve D is generated with $c_1 = -0.22\mu^{-3}$ that was obtained by fitting to the π^--^{208}Pb atom data with the realistic ρ_n. Curve D corresponds to a consistent calculation using the realistic ρ_n. Curves B, C, and D are indeed rather close to each other. This realistic ρ_n has the two-parameter Fermi distribution form with the density parameter values $(c, t) = (6.88$ fm, 2.30 fm) which closely simulates Negele's density-dependent Hartree-Fock density.

From these computations for the π^+-^{208}Pb scattering we see that the original disagreement of curve A with the data at the dip is mainly due to a poor determination of b_1 which was originated in

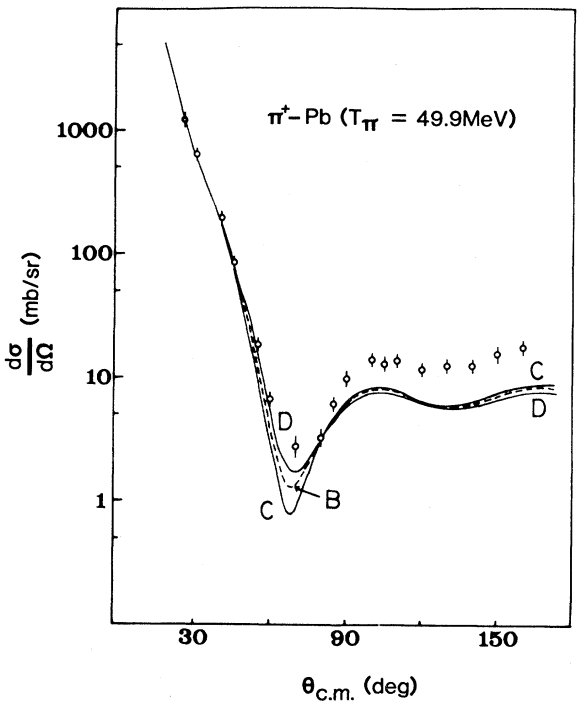

FIG. 9. Effect of the use of a realistic ρ_n $[\neq(N/Z)\rho_p]$ on π^+-^{208}Pb scattering at 49.9 MeV. Curve B is identical to curve B in Fig. 8. Curves D and C are calculated using ρ_n of a two-parameter Fermi distribution form which simulates Negele's density dependent Hartree-Fock neutron density of ^{208}Pb. The potential parameters used are the same as or close to those used for curve B. Curve D corresponds to the most consistent use of the realistic ρ_n. (See the text for details.) The data are from Ref. 15.

the π^--atom analysis. The disagreement at the dip is certainly not because of our neglect of the Lorentz-Lorenz effect or any other detailed structure of the potential. We present further evidence of this statement in Fig. 10. The figure shows three curves computed from the potentials which have the nonlocal ρ^2 term with positive (A), zero (B), and negative (C) coefficients, respectively. These potentials are chosen in a way that they are effectively equivalent, as discussed in the preceding paper. That is, the nonlocal parts of these potentials are related via

$$(\mathrm{Re}c)\rho(r) = \mathrm{Re}(c' + C\rho_e)\rho(r) \rightarrow \mathrm{Re}[c'\rho(r) + C\rho^2(r)] ,$$

using the effective density ρ_e for the π^+-^{208}Pb scattering at 50 MeV. Here c, c', and C are sums of the isoscalar and isovector parts for the π^+-^{208}Pb interaction. Despite the ρ^2 term with different signs, three curves agree closely with the data. The disagreement at the dip is not certainly an indication of the limitation of our approach.

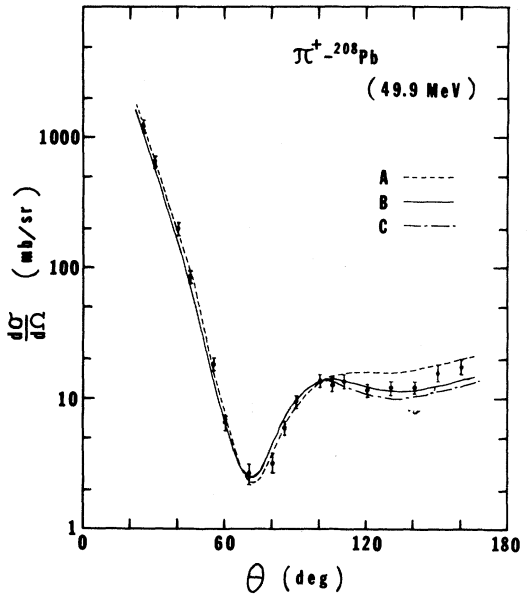

FIG. 10. The best-fit π^+-^{208}Pb cross sections at 49.9 MeV using potential parameters which give the same effective values. The potential form used is the KIS with an additional nonlocal term $\vec{\nabla}\,\mathrm{Re}C\rho^2(r)\cdot\vec{\nabla}$. Re$C$ is varied as $-0.465\mu^{-6}$ (the corresponding cross sections shown as curve A), zero (curve B), and $+0.155\mu^{-6}$ (curve C). For these values of ReC the value of c is adjusted so that $\mathrm{Re}(c+C\rho_e)$ remains about the same, $-0.18\mu^{-3}$. The χ^2 value is varied as 36.2, 19.4, and 33.4 for these combinations of ReC and Rec, respectively. (ReC=0 is just about the best fit.) The densities used obey the assumption $\rho_n/N=\rho_p/Z$.

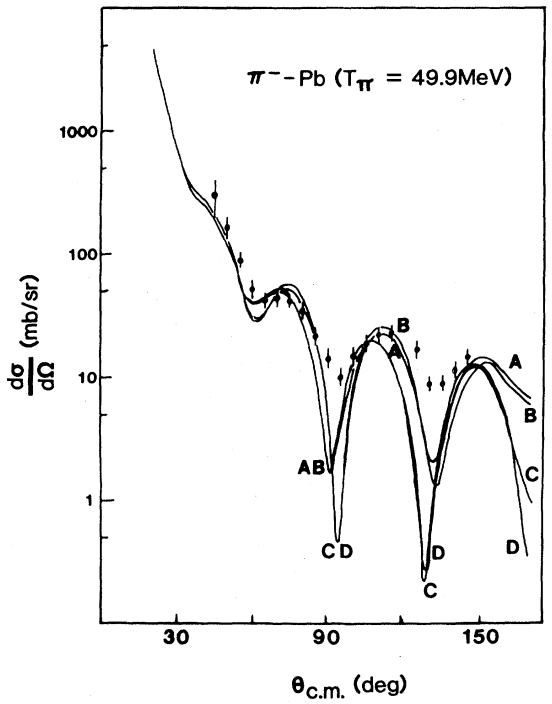

FIG. 11. Effects of the new b_1 value and of the use of a realistic ρ_n on π^--^{208}Pb scattering at 50 MeV. Curves A–D are obtained in the same way as described in Figs. 8 and 9. Curves C and D, in which the realistic ρ_n is used, are noticeably different from the other curves in which the ρ_n [$=(N/Z)\rho_p$] is used. The data are at 50 MeV from Ref. 23.

Our calculations so far described demonstrate a usefulness of analyses in which π^- (atom or scattering) data and π^+ scattering data are combined. The reason for this is two groups of the data yield information about the optical potential with different signs of the isovector parts: As seen in Eq. (1) and Tables I–III, isoscalar and isovector parameters have the same sign in both the local and nonlocal parts of the potential for the π^- interaction, but the parameters have opposite signs for the π^+ interaction.

We have repeated the above computations of curves A–D also in the case of the π^--^{208}Pb scattering. Figure 11 illustrates these curves in this case. The major difference between this π^- case and the previous π^+ case lies in the fact that a different choice of ρ_n, not of b_1, makes the cross sections different in the π^- case, while a choice of b_1, not of ρ_n, makes a difference in the π^+ case. In Fig. 11, curves A and B are close, and curves C and D are close, forming two groups of curves. The sensitivity of the π^- scattering to ρ_n has recently been exploited to extract a difference of the neutron RMS radii between isotopes.[24] Using the idea of the effective density, we presented at the end of the preceding paper an explanation of why this particular method may be reliable despite the seemingly many parameters involved.

Closing this section, we make a pertinent technical comment. During the investigation of the dip in the π^+-^{208}Pb scattering at 50 MeV, we realized that the nonrelativistic treatment of the Coulomb potential in the Klein-Gordon equation is partially responsible for the dip being much deeper than that observed. The Coulomb potential near the nuclear surface of ^{208}Pb reaches about 15 MeV and the relativistic correction of the quadratic Coulomb potential term is no longer negligible. We remedied this problem basically by applying the method of Cooper, Jeppesen, and Johnson[25] except that we actually computed the low-partial-wave contribution by numerically integrating out to a reasonably large distance.

V. DISCUSSION AND CONCLUSION

During the course of this work we encountered a subtle ambiguity in our hybrid method of the extrapolation from the threshold to a scattering energy T_π ($\lesssim 50$ MeV). The effect of the ambiguity turns out to be roughly the same size as the effect due to the choice of ρ_n in the π^+ scattering discussed in the previous section, and thus the ambiguity is not a very serious problem. However, it does indicate a limitation of our approach, the method of the effective nuclear density, and it deserves some discussion.

In the calculation described in the preceding sections, we have used the value of the effective density only at the threshold, $\rho_e(0)$, in the computation of the energy-dependence corrections, $\Delta(T_\pi)$. Here ρ_e was regarded to be independent of T_π, but it actually increases slowly as T_π increases, as described in the preceding paper. If one tries to include explicitly the T_π dependence in ρ_e so as to compute the potential parameters consistently, one must know the detailed structure of the potential and how its parameters depend on T_π. In the absence of such knowledge one has to make some assumptions, and assumptions create ambiguity.

Let us use a concrete example. Instead of $\Delta(T_\pi)$ of Eq. (4) we could use

$$\Delta'(T_\pi)=b_0^c(T_\pi,\rho_e(T_\pi))-b_0^c(0,\rho_e(0)) , \tag{5}$$

which differs from $\Delta(T_\pi)$ in the use of $\rho_e(T_\pi)$ in the first b_0^c. This choice is equivalent to the relation

$$\delta(T_\pi)=\delta(0) , \tag{6}$$

where

$$\delta(T_\pi)=b_0(T_\pi)-b_0^c(T_\pi,\delta_e(T_\pi)) ,$$

$$\delta(0)=b_0(\text{atom})-b_0^c(0,\delta_e(0)) .$$

That is, δ is what is missing in b_0^c compared with the true b_0, and Eq. (6) states that it is independent of T_π. Now, b_0^c was computed as the π-nucleon scattering amplitude in the nuclear medium without any correction arising from reaction processes, of which the major process is the π absorption. Therefore, Eq. (6) is the same statement as that we neglect the energy dependence of the π absorption when its effect is interpreted as potential terms proportional to $\rho(r)$. It is a difficult task to justify this statement because, in order to do it, we have to have a (nearly) complete microscopic theory of the potential. Let us elaborate on this: The effect of the π absorption is interpreted using the effective nuclear density ρ_e, but in order to interpret it properly we must know the value of ρ_e at T_π and how the coefficients of $\rho^2(r)$ depend on ρ_e. That is, the requirements for the proper interpretation are a thorough understanding of microscopic theory of the potential (so that we know how the coefficients depend on ρ_e) and a phenomenological analysis using the potential (so that we know the value of ρ_e). Once we know this much, the benefit of using ρ_e is only that it is a convenient language of bookkeeping.

Thus we see that without further microscopic knowledge it is hard to judge which of $\Delta(T_\pi)$ and $\Delta'(T_\pi)$ is appropriate and therefore the choice becomes an ambiguity of our method. In this paper we used $\Delta(T_\pi)$ for simplicity because it requires only $\rho_e(0)$. [As seen below, this $\rho_e(0)$ can be replaced by $\rho_e(T_\pi)$ of any T_π with little numerical change in the results.]

In Table II we compare Δ (50 MeV) and Δ' (50 MeV) for all potential parameters. We see that Δ and Δ' for $\mathrm{Re}b_0$ and $\mathrm{Re}c_0$ are particularly larger than for other parameters and differ noticeably from each other. We therefore illustrate in Fig. 12 how

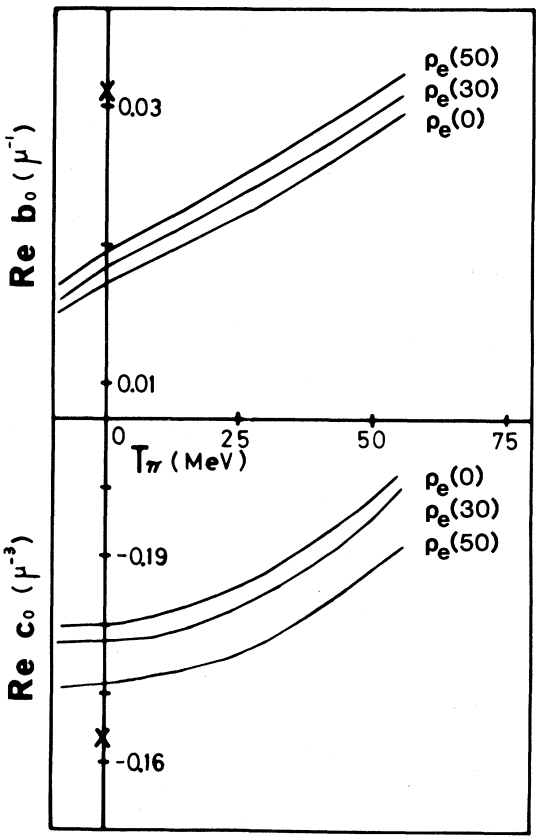

FIG. 12. The calculated potential parameters b_0^c and c_0^c using various values of the effective density. (See the text for details.) x indicates the phenomenological threshold value determined from the π^--atom data. The major contribution to the difference between x and the calculated value at the threshold comes from the π absorption process.

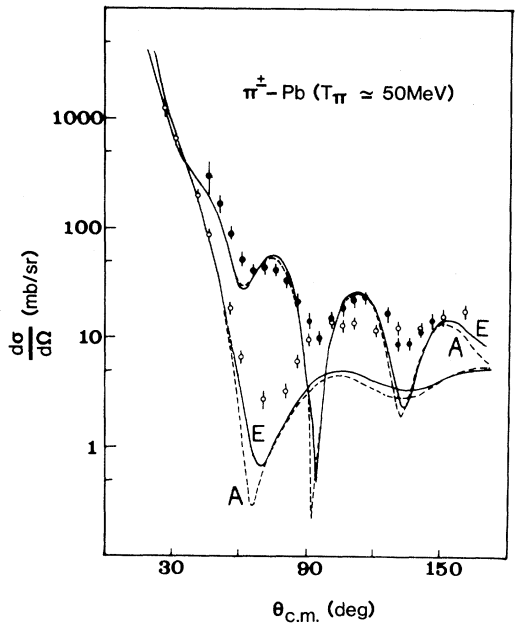

FIG. 13. Effect of the choice of either $\Delta(T_\pi)$ or $\Delta'(T_\pi)$ on $\pi^{\pm}$-^{208}Pb scatterings at 50 MeV. Curve A is the same as curve A in Fig. 8; that is, it is obtained using $\Delta(T_\pi)$. Curve E is calculated using $\Delta'(T_\pi)$ under the same conditions.

different $b_0^c(T_\pi,\rho_e)$ and $c_0^c(T_\pi,\rho_e)$ depend on the choice of ρ_e. This figure indicates the degree of ambiguity contained in our calculation. Note that the figure shows that b_0^c and c_0^c as functions of T_π simply shift up or down when a different ρ_e is chosen. Therefore, if $\rho_e(0)$ is replaced by, say, ρ_e (50 MeV) in both terms of $\Delta(T_\pi)$ of Eq. (4), $\Delta(T_\pi)$ remains roughly the same numerically. This provides extra convenience for using $\Delta(T_\pi)$ because we are free to choose ρ_e at any energy as long as it is used in both terms of $\Delta(T_\pi)$.

In Fig. 13 we illustrate how actually different the $\pi^{\pm}$-^{208}Pb cross sections are by the choice of $\Delta(T_\pi)$ or $\Delta'(T_\pi)$. The cross sections do not differ much by different choices, but in the case of π^+ the difference is roughly the same size as the consequence of different choices of ρ_n shown in Fig. 9. As discussed above, this difference indicates how well we can describe the scattering data without knowing the energy dependence of the reaction processes.

In conclusion, within the above limitation, our method of using the effective nuclear density works well and the calculations shown demonstrate that it is a useful way to describe the low-energy π-nucleus elastic scattering. In view of the fact that the number of potential parameters is kept at a minimum (contrary to the work of other authors), we believe that our calculations show the energy dependence correction, after the Pauli-blocking the Fermi-averaging effects are included, to be the crucial microscopic corrections for the extrapolation from the threshold to a low (scattering) energy. We find that the angular transformation terms also play the crucial role in the extrapolation. However, the calculations do *not* show that other complicated features of the potential such as the Lorentz-Lorenz effect or some highly nonlocal effects are essential for the extrapolation.

ACKNOWLEDGMENTS

We acknowledge useful discussions with many colleagues on various occasions over the years during which this work was carried out. A part of the work was carried out at the Lawrence Berkeley Laboratory during the summers of 1979 and 1980. One of us (R.S.) thanks Professor Owen Chaimberlain and Professor Clyde Wiegand for continued warm hospitality and also thanks the Associated Western Universities for support. As in the preceding paper, we used our modified version of a computer code FITPI in the analysis of the scattering data. We thank Dr. M. D. Cooper and Professor R. A. Eisenstein for supplying us with the original FITPI and for allowing us to modify it. This work was also supported in part by the DOE under Contract No. DE-AC03-82ER40071 at California State University, Northridge, and by the National Science Foundation under Grant No. PHY79-23638 at California Institute of Technology.

APPENDIX A: EVALUATION OF EQUATION (2)

We evaluate Eq. (2) first by including the Pauli-blocking effect in the Fermi gas model. Equation (2) becomes

$$\tau(\vec{k}',\vec{k};\vec{K},E)=t(\vec{k}',\vec{k};E)-\int\frac{d^3k''}{(2\pi)^3}t(\vec{k}',\vec{k}'';E)Q(\vec{k}'',\vec{K})G_0(\vec{k}'',E)\tau(\vec{k}'',\vec{k};\vec{K},E)\,, \tag{A1}$$

where $Q(\vec{k}'',\vec{K})$ describes the effect of the Pauli exclusion principle and is

$$Q(\vec{k}'',\vec{K})=\begin{cases}1 & \text{for } |\xi\vec{K}-\vec{k}''| \le p_F \\ 0 & \text{for } |\xi\vec{K}-\vec{k}''| > p_F\end{cases} \tag{A2}$$

in terms of the Fermi momentum p_F and $\xi \equiv m/(m+W)$ with $W\,(=T_\pi+\mu)$ the pion energy. Here $\vec{k}$'s are the π-nucleon relative momenta. $\vec{K}$ is the total momentum of the π-nucleon system, and E is the π-nucleon c.m. total energy. Note that in our on-the-mass-shell problem E is not an independent parameter because it is fixed once $\vec{k}$ is given. $G_0(\vec{k},E)$ is expressed as either "a relativistic Schrödinger form"

$$G_0^{-1}(\vec{k},E)=E-m-\vec{k}^2/2m-(\vec{k}^2+\mu^2)^{1/2}+i\epsilon\,, \tag{A3}$$

or "a Klein-Gordon form"

$$G_0^{-1}(\vec{k},E)=(E-m-\vec{k}^2/2m)^2-(\vec{k}^2+\mu^2)+i\epsilon\,, \tag{A4}$$

where (in both forms) the nucleon is treated nonrelativistically and $\epsilon\to+0$. Since $Q(\vec{k}'',\vec{K})$ depends on an angle between $\vec{k}''$ and $\vec{K}$, Eq. (A1) becomes (infinite) coupled equations when the equation is decomposed in partial waves. We therefore average $Q(\vec{k}'',\vec{K})$ over this angle:

$$Q(\vec{k}'',\vec{K})\to Q_0(\vec{k}'',\vec{K})=\begin{cases}1 & \text{for } \xi K+k''\le p_F \\ 0 & \text{for } |\xi K-k''| < p_F \\ [p_F^2-(\xi K-k'')^2]/4\xi K k'' & \text{otherwise}\,.\end{cases} \tag{A5}$$

Let us apply these expressions to the nuclear matter ($N=Z$) so that $Q(\vec{k}'',\vec{K})$ is independent of the isospin, and each isospin component of Eq. (A1) does not couple with others. Substituting Eqs. (A3) and (A5) into Eq. (A1), we obtain for the s wave,

$$\bar{a}(\vec{K},E)=a(E)\left\{1-\frac{a(E)}{\pi}\int\frac{k^2dk}{\omega}Q_0(\vec{k},\vec{K})G_0(\vec{k},E)\right\}^{-1} \tag{A6}$$

for which we used

$$t(\vec{k}',\vec{k};E)=-4\pi a(E)/2(\omega'\omega)^{1/2}\,,$$
$$\tau(\vec{k}',\vec{k};\vec{K},E)=-4\pi\bar{a}(\vec{K},E)/2(\omega'\omega)^{1/2}\,, \tag{A7}$$

Here $\omega=(\vec{k}^2+\mu^2)^{1/2}$ and $\omega'=(\vec{k}'^2+\mu^2)^{1/2}$.

For the p wave, we obtain similarly

$$\bar{a}(\vec{K},E)=a(E)\left\{1-\frac{a(E)}{\pi}\int\frac{k^4dk}{\omega}Q_0(\vec{k},\vec{K})G_0(\vec{k},E)\right\}^{-1}\,, \tag{A8}$$

for which we used

$$t(\vec{k}',\vec{k};E)=-4\pi\cdot 3a(E)\vec{k}'\cdot\vec{k}/2(\omega'\omega)^{1/2}\,,$$
$$\tau(\vec{k}',\vec{k};\vec{K},E)=-4\pi\cdot 3\bar{a}(\vec{K},E)\vec{k}'\cdot\vec{k}/2(\omega'\omega)^{1/2} \tag{A9}$$

after an angular average

$$\vec{k}'\cdot\vec{k}''\vec{k}''\cdot\vec{k}\to\tfrac{1}{3}k''^2(\vec{k}'\cdot\vec{k})\,.$$

When the Klein-Gordon form, Eq. (A4), is used instead of the relativistic Schrödinger form, Eq. (A3), 2ω and $2\omega'$ are replaced by unity in Eqs. (A6)–(A9).

Finally we average $\bar{a}(\vec{K},E)$'s over the initial nucleon laboratory momentum in the Fermi gas so as to include the effect of the Fermi motion. As a consequence, $\bar{a}$'s become functions of only T_π. These Fermi-averaged $\bar{a}$'s are related to the potential parameters as $-p_1 b_0$, etc., when the impulse approximation in the lowest order of nuclear density expansion is applied. In the actual numerical calculation we computed $\bar{a}$'s using the Klein-Gordon form of $G_0(\vec{k},E)$, Eq. (A4), though we observed little difference in numerical results using the two forms in our energy range.

APPENDIX B: THE DISAPPEARANCE OF THE THRESHOLD CUSP IN THE BOUND π-NUCLEON AMPLITUDE

The disappearance of the s-wave threshold cusp in the lowest order of the π-nucleus relative momentum, k, is due to the Pauli exclusion principle and is

a general property of the scattering amplitude in the nuclear medium. In our actual calculation we do include the nucleon recoil effect and Fermi motion of the nucleon. Consequently the bound π-nucleon amplitude is expressed in terms of a complicated integral and has to be evaluated numerically, as can be seen in Appendix A. If we were to ignore these effects, the amplitude could be expressed analytically and the disappearance of the threshold cusp could be demonstrated explicitly. In this appendix we show such a simplified expression of the amplitude in order to demonstrate and elucidate the disappearance of the cusp at the threshold. To be explicit, we use in the evaluation of the propagators the following approximations: (1) neglect of the nucleon recoil energy (i.e., a static approximation); (2) neglect of the initial pion momentum compared to the initial nucleon momentum; and (3) neglect of the coupling among partial waves which arises from the use of $Q(\vec{k}'',\vec{K})$ of Eq. (A2) rather than of $Q_0(\vec{k}'',\vec{K})$ of Eq. (A5). By use of the Klein-Gordon form of $G_0(\vec{k},E)$, Eq. (A1) then becomes for the s wave

$$-4\pi\bar{a}(\omega)=-4\pi a(\omega)+(-4\pi)^2\bar{a}(\omega)a(\omega)\int\frac{d^3p\,d^3p'}{(2\pi)^6}\frac{\{\theta(p'-p_F)-1\}\theta(p_F-p)}{\omega^2-\mu^2-(\vec{p}-\vec{p}\,')^2+i\epsilon}\Big/\int\frac{d^3p}{(2\pi)^3}\theta(p_F-p)\,, \tag{B1}$$

where $\theta(x)=1$ for $x\geq 0$, or 0 for $x<0$ is the step function, and $\vec{p}$ and $\vec{p}\,'$ are the initial and intermediate nucleon momenta, respectively, in the laboratory system. This equation yields

$$\bar{a}(\omega)=a(\omega)\{1+\eta(\omega)a(\omega)\}^{-1}\,, \tag{B2}$$

where for $\omega\geq\mu$

$$\eta(\omega)=\frac{3}{2\pi}p_F\left[1-\tfrac{4}{3}\left\{\beta\ln\left|\frac{1+\beta}{1-\beta}\right|+\tfrac{1}{2}\beta^2(\beta^2-3)\ln\left|\frac{\beta^2}{1-\beta^2}\right|-\tfrac{1}{2}\beta^2\right\}+i\frac{4\pi}{3}\beta\left\{1-\tfrac{3}{2}\beta+\tfrac{1}{2}\beta^3\right\}\theta(1-\beta)\right]\,, \tag{B3}$$

and for $\omega<\mu$

$$\eta(\omega)=\frac{3}{2\pi}p_F\left[1-\tfrac{4}{3}\left\{2\beta'\tan^{-1}\frac{1}{\beta'}-\tfrac{1}{2}\beta'^2(\beta'^2+3)\ln\left[\frac{1+\beta'^2}{\beta'^2}\right]+\tfrac{1}{2}\beta'^2\right\}\right]\,. \tag{B4}$$

Here

$$\beta\equiv(\omega^2-\mu^2)^{1/2}/2p_F$$

and $\beta'\equiv|\beta|$. Upon evaluating ω, we neglect the nucleon energy and thus $\beta=k/2p_F$ in terms of the pion-nucleus c.m. momentum, k. Near the threshold, $\beta\to 0$, η thus behaves as

$$\eta(k)=\frac{3}{2\pi}p_F+ik+\mathcal{O}(k^2)\,. \tag{B5}$$

Since near the threshold a behaves as

$$a(K)=[A^{-1}-ik+\mathcal{O}(k^2)]^{-1} \tag{B6}$$

in terms of the scattering length A, we observe that $+ik$ in Eqs. (B5) and (B6) cancel each other when these equations are substituted into Eq. (B2). $\bar{a}(k)$ then behaves as

$$\bar{a}(k)=\left[A^{-1}+\frac{3}{2\pi}p_F+\mathcal{O}(k^2)\right]^{-1}\,, \tag{B7}$$

which does not contain the nonanalytic term, $+ik$, and has no prominent cusp near the threshold.

In the case of the p wave we can also prove in the same manner that the nonanalytic term, $+ik$, in $a(k)$ cancels the similar term in $\eta(k)$, and consequently $\bar{a}(k)$ is analytic in the lowest order of k. The p-wave cusp in $a(k)$ is generally not prominent, but this cancellation makes it negligible in $\bar{a}(k)$.

Let us make two comments: (1) The leading term in Eq. (B5) for the s wave and a similar term for the p wave agrees with the expressions given by Hüfner[26]; (2) the analytic expressions thus obtained generally yield results very close to those calculated by the more elaborate numerical method of Appendix A without the above three approximations. Exceptions occur for the imaginary parts of the p-wave parameters, as discussed in the main text.

*Present address: SIN, Villigen, CH-5234, Switzerland.
[1]G. G. Bunatyan and Yu. S. Pol', Yad. Fiz. 25, 535 (1977) [Sov. J. Nucl. Phys. 25, 287 (1977)].
[2]K. Stricker, H. McManus, and J. A. Carr, Phys. Rev. C 19, 929 (1979).
[3]K. Stricker, J. A. Carr, and H. McManus, Phys. Rev. C 22, 2043 (1980).
[4]M. Ericson and T. E. O. Ericson, Ann. Phys. (N.Y.) 36, 323 (1966).
[5]M. Thies, Phys. Lett. 63B, 43 (1976), and references therein; G. A. Miller, Phys. Rev. C 10, 1242 (1974), and references therein.
[6]R. Seki and K. Masutani, Phys. Rev. C 27, 2799 (1983), the preceding article.
[7]R. Seki, K. Masutani, M. Oka, and Y. Yazaki, abstracts of contributed papers to the 8th International Conference on High Energy Physics and Nuclear Structure, TRIUMF and the University of British Columbia, 1979, pp. 23, 24.
[8]R. Seki, K. Masutani, M. Oka, and K. Yazaki, Phys. Lett. 97B, 20 (1980).
[9]C. J. Batty *et al.*, Phys. Rev. Lett. 40, 931 (1978); Nucl. Phys. A322, 445 (1979); A355, 383 (1981).
[10]R. H. Landau and A. W. Thomas, Nucl. Phys. A302, 461 (1978).
[11]G. Rowe, M. Salomon, and R. H. Landau, Phys. Rev. C 18, 584 (1978).
[12]R. D. Amado, F. Lenz, and R. Yazaki, Phys. Rev. C 18, 918 (1978); R. S. Bhalerao, L. C. Liu, and C. M. Shakin, *ibid.* 21, 2103 (1980).
[13]M. A. Moinester *et al.*, Phys. Rev. C 18, 2678 (1978).
[14]R. R. Johnson *et al.*, Nucl. Phys. A296, 444 (1978).
[15]B. M. Preedom *et al.*, Phys. Rev. C 23, 1134 (1981).
[16]R. R. Johnson *et al.*, Phys. Lett. 78B, 560 (1978).
[17]M. Blecher *et al.*, Phys. Rev. C 20, 1884 (1979).
[18]I. Schwanner *et al.*, Phys. Lett. 96B, 268 (1980).
[19]A. Olin *et al.*, Nucl. Phys. A312, 361 (1978); A360, 426 (1981); C. A. Fry *et al.*, *ibid.* A375, 325 (1982); B. H. Olaniyi *et al.*, *ibid.* A384, 345 (1982).
[20]E. Friedman and A. Gal, Nucl. Phys. A345, 457 (1980).
[21]E. Friedman, Phys. Lett. 104B, 357 (1981).
[22]C. J. Batty *et al.*, Nucl. Phys. A322, 445 (1979).
[23]R. R. Johnson *et al.*, Can. J. Phys. 57, 775 (1979).
[24]A. W. Thomas, Nucl. Phys. A345, 51 (1981).
[25]M. D. Cooper, R. H. Jeppesen, and M. B. Johnson, Phys. Rev. C 20, 696 (1979).
[26]J. Hüfner, Phys. Rep. 21, 1 (1975).